

Integrated Circuits for Volumetric Ultrasound Imaging With 2-D CMUT Arrays

Anshuman Bhuyan, *Student Member, IEEE*, Jung Woo Choe, *Student Member, IEEE*,
Byung Chul Lee, *Student Member, IEEE*, Ira O. Wygant, *Member, IEEE*, Amin Nikoozadeh, *Member, IEEE*,
Ömer Oralkan, *Senior Member, IEEE*, and Butrus T. Khuri-Yakub, *Fellow, IEEE*

Abstract—Real-time volumetric ultrasound imaging systems require transmit and receive circuitry to generate ultrasound beams and process received echo signals. The complexity of building such a system is high due to requirement of the front-end electronics needing to be very close to the transducer. A large number of elements also need to be interfaced to the back-end system and image processing of a large dataset could affect the imaging volume rate. In this work, we present a 3-D imaging system using capacitive micromachined ultrasonic transducer (CMUT) technology that addresses many of the challenges in building such a system. We demonstrate two approaches in integrating the transducer and the front-end electronics. The transducer is a 5-MHz CMUT array with an 8 mm \times 8 mm aperture size. The aperture consists of 1024 elements (32×32) with an element pitch of 250 μ m. An integrated circuit (IC) consists of a transmit beamformer and receive circuitry to improve the noise performance of the overall system. The assembly was interfaced with an FPGA and a back-end system (comprising of a data acquisition system and PC). The FPGA provided the digital I/O signals for the IC and the back-end system was used to process the received RF echo data (from the IC) and reconstruct the volume image using a phased array imaging approach. Imaging experiments were performed using wire and spring targets, a ventricle model and a human prostate. Real-time volumetric images were captured at 5 volumes per second and are presented in this paper.

Index Terms—2D array, capacitive micromachined ultrasonic transducer (CMUT), flip-chip bonding, integrated circuits, phased array imaging, ultrasound, volumetric imaging.

I. INTRODUCTION

3-D ultrasound imaging is becoming increasingly prevalent in the medical field [1], [2]. Compared to conventional 2-D imaging systems, 3-D imaging systems provide a detailed view of tissue structures that make diagnosis easier for the physicians. In addition, since the 2-D image slices can be formed at various orientations, the examination is less dependent on the skill of the sonographer. Finally, 3-D volume images also make great

Manuscript received October 15, 2013; revised December 04, 2013; accepted December 23, 2013. Date of publication January 17, 2014; date of current version January 28, 2014. This work was supported by the National Institute of Health Grant 5R01CA134720. Texas Instruments and Intersil provided support for fabrication of the ICs. This paper was recommended by Associate Editor P. Mercier.

A. Bhuyan, J. W. Choe, B. C. Lee, A. Nikoozadeh, and B. T. Khuri-Yakub are with the Edward L. Ginzton Laboratory, Stanford University, Stanford, CA 94305 USA (e-mail: anshu@stanford.edu).

I. O. Wygant is with Texas Instruments, Sunnyvale, CA 94089 USA.

Ö. Oralkan is with the Electrical Engineering Department, North Carolina State University, Raleigh, NC 27606 USA.

Color versions of one or more of the figures in this paper are available online at <http://ieeexplore.ieee.org>.

Digital Object Identifier 10.1109/TBCAS.2014.2298197

utility for offline analyses after the examination is done, and reduces repeat examination making it more cost-effective to the patient.

Early 3-D imaging systems consisted of mechanically scanned 1-D arrays [3] or sparsely populated 2-D arrays [4]. Newer systems, however, use fully populated 2-D arrays as the increased number of elements improves the image resolution, contrast and SNR [5]. 2-D arrays also provide better imaging frame rate as compared to a mechanically scanned 1-D array and allow focusing in both the azimuth as well as the elevation plane. There are, however, various challenges in developing a 3-D imaging system for a fully populated 2-D array; such as fabrication of a large 2-D array and integration of a large number of elements to the back-end system. Having long cables (usual capacitances of 100 pF/m) going from the transducer element to the system will also degrade SNR and receive sensitivity. 2-D array elements are usually smaller than 1-D array elements and have smaller capacitance (in the order of few picofarads) making them more susceptible to parasitic capacitance. Finally, a large number of 2-D transducer array elements would require a large number of cables to the back-end system making the hand-held probe very bulky. A large number of dataset would also need to be processed, possibly degrading the imaging frame rate.

One way to mitigate the issue is to closely integrate the transducer array with the electronics [6]–[8]. The literature contains numerous integrated circuit designs for ultrasound applications. These include transmit beamformers, ADCs, analog receive beamformers as well as switching circuitry for multiplexing multiple transducer array [9]–[16]. Having the integrated circuit close to the transducer enables us to reduce the post-processing burden on the back-end system and the cabling by incorporating partial beamforming in the IC.

We use capacitive micromachined ultrasonic transducer (CMUT) arrays as our ultrasonic transducer. CMUTs provide several advantages over piezoelectric transducers; CMUTs inherently provide wide bandwidth, which translates to better axial resolution, without a need for matching layers. They benefit from MEMS fabrication and batch processing leading to design flexibility, fabrication precision and reproducibility, and reduced manufacturing cost. The capability to seamlessly incorporate through-wafer interconnects with CMUTs, allows for their easy integration with supporting electronics.

Previous research presents different ways to integrate the CMUT and the electronics. There is the monolithic approach where the CMUT is fabricated on top of the electronics by

post-processing/co-processing the same wafer used for IC fabrication [17]. Another approach is the multi-chip approach where one would fabricate the CMUT and the IC on separate wafers and integrate them using flip-chip bonding technology [18]. We prefer the second approach as it allows us for optimization of both the CMUT and the IC during fabrication without compromising the other. It may also not necessarily be area-efficient to fabricate the CMUT and the IC on the same wafer.

In this paper, we present a fully functional 3-D ultrasound imaging system using 2-D CMUT arrays. We developed integrated circuits that are 3-D stacked with the transducer array using flip-chip bonding technology. The imaging system is capable of capturing real-time volumetric ultrasound data and displaying 2-D and 3-D ultrasound images. We first discuss the approach in integrating our CMUT and ICs. Then we describe our IC design in detail. After that, we explain our imaging setup and finally provide imaging results of wire and spring targets, ventricle model, and a human prostrate (*ex-vivo*).

II. SYSTEM DESIGN CONSIDERATIONS

We demonstrate two approaches in developing the front-end system, comprising of the transducer and the integrated circuits. The first approach is to tile several small transducer arrays to form a larger array and integrate them with the circuits. Due to the different pitch of the transducer array and the IC, this approach requires an interposer layer that acts as a fan-out board between the transducer array and the IC. We use this approach to tile four 16×16 -element CMUT arrays to form a 32×32 -element array and integrate them with multiple ICs.

The second approach is to directly integrate a single CMUT array to a single integrated circuit. In this case, the CMUT and the IC arrays must have identical pitch between the elements to enable direct flip-chip bonding. We demonstrate this approach by integrating a 32×32 CMUT array directly on top of a 32×32 IC.

Both approaches have their advantages and disadvantages and the appropriate choice between them would be made based on the targeted application. Often times, the IC die cannot be scaled to the size of the transducer array due to the limitation in the foundry's reticle size and therefore, application that requires a large aperture would benefit from the first approach. On the other hand, the second approach allows us to build imaging probes that have a very small form factor benefiting application such as cardiac imaging.

In both approaches, we developed ICs that are capable of performing transmit beamforming. The transmit pulse amplitude is in the range of 25 V–60 V. For the 32×32 IC, we also incorporated an additional multi-beam transmit feature that allows simultaneous transmit of up to four beams. The multi-beam feature will allow us to improve the frame rate by about 4 times without much degradation in image quality. Interference between the multiple beams can be eliminated by intelligently grouping the beams transmitted together (for example, main lobe of a beam falling into the null of the other beams can be transmitted together). These ICs also contain RX channels with low-noise amplifiers to signal condition the receive signal from the CMUT. In the rest of the paper, we refer to the devices based

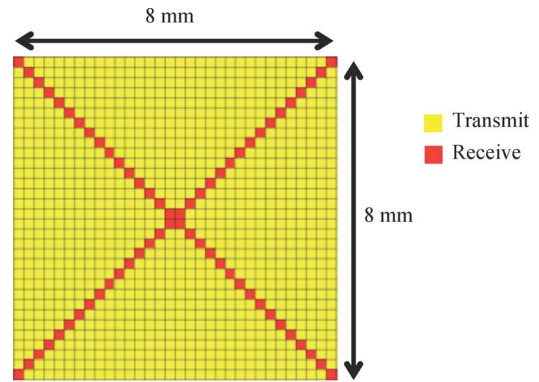


Fig. 1. 32×32 array aperture.

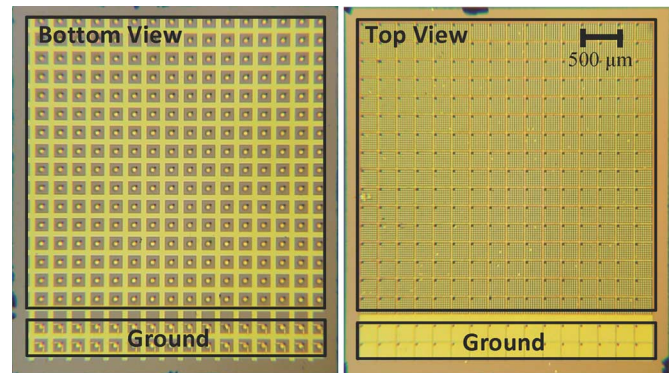


Fig. 2. 16×16 CMUT array.

on the first and second assembly approaches as “Assembly A” and “Assembly B”, respectively.

The imaging aperture for both approaches is shown in Fig. 1. It consists of 1024 elements and measures $8 \text{ mm} \times 8 \text{ mm}$. The 64 diagonal elements are used for receive while the remaining 960 elements are used for transmit of the ultrasound beam. Since the number of RF cable connections to the imaging system increases with the number of receive channels, it is desirable to reduce the number of receiving elements. Previous study [19] analyzed different transmit and receive configuration for a 2-D array and the presented configuration (Fig. 1) resulted in the best compromise between the number of receiving elements and image quality. As described in that paper, the SNR degradation from using only diagonal elements as receive (versus the entire aperture) is about 12 dB.

Our CMUT arrays (Fig. 2) have been fabricated using the sacrificial release process described in [20]. The CMUT plate and cavity dimensions were chosen based on a combination of the CMUT equivalent circuit, analytical circuit model and finite element modeling [21]–[23]. These transducers have an operating center frequency of 5 MHz and an element-to-element pitch of $250 \mu\text{m}$. The pull-in voltage for the 16×16 and 32×32 CMUT arrays is 36 V and 40 V respectively.

Since a large number of elements need to interconnect to the IC, flip-chip bonding is used as a means for integration. Therefore, through-silicon-vias are incorporated in the CMUT array to allow for backside access to each and every element. The fabrication of these vias in our CMUTs is described in [24], [25].

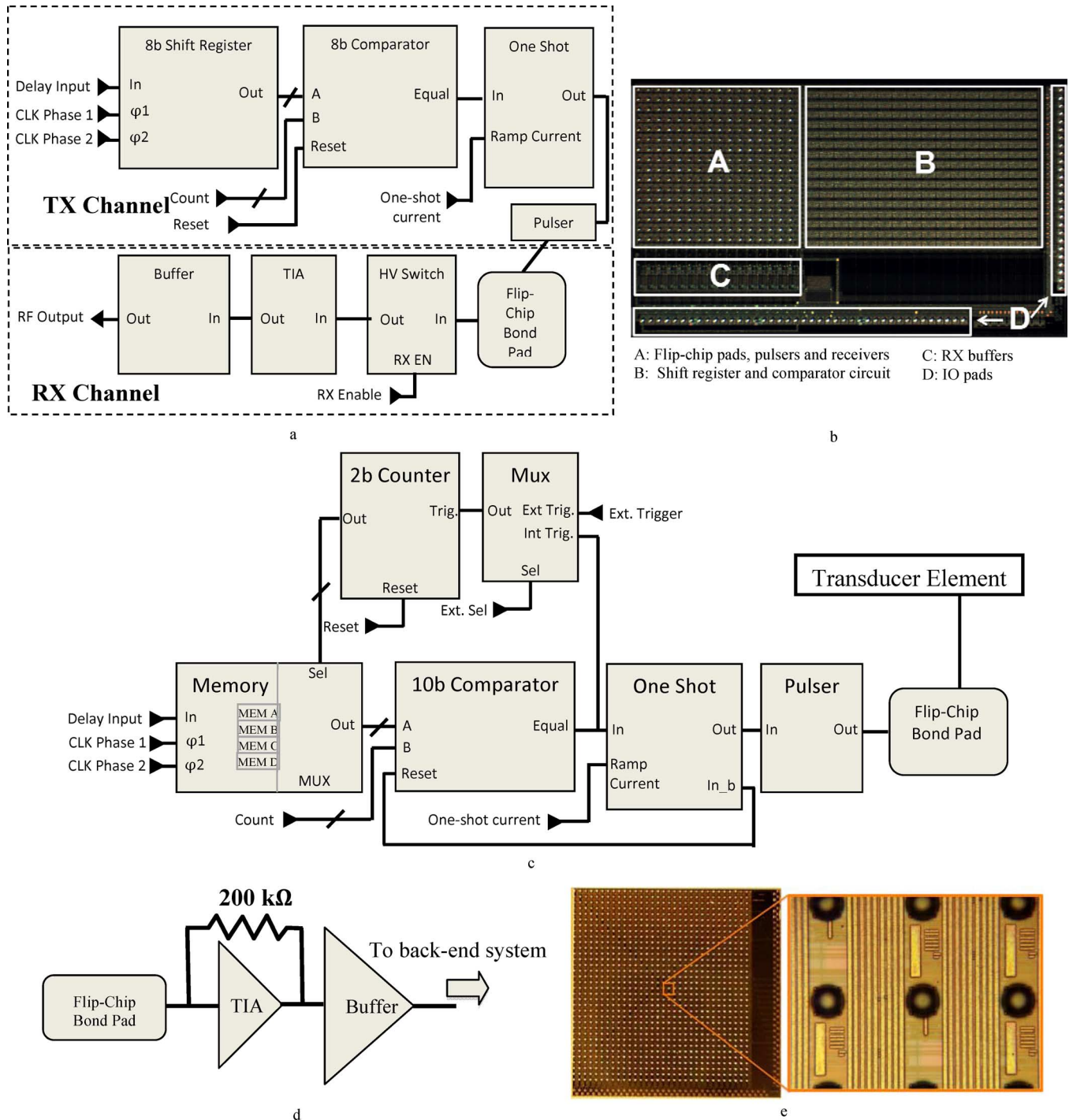


Fig. 3. (a) 16×16 IC block diagram. (b) 16×16 IC die photo (10 mm \times 6 mm). (c) 32×32 IC transmit block diagram. (d) 32×32 IC receive block diagram. (e) 32×32 IC die photo (9.2 mm \times 9.2 mm).

III. IC DESIGN

A. 16×16 IC

For Assembly A, we use four 16×16 ICs that have been fabricated in a $1.5\text{-}\mu\text{m}$ high-voltage process. This IC is a slightly modified version of the one described in [6]. The IC consists of 256 elements that are capable of interfacing 256 CMUT elements for transmit and receive. The block diagram of a single element is shown in Fig. 3(a). The transmit circuitry is capable

of generating focused ultrasound beams and consists of an 8-bit shift register, a comparator, a one-shot circuit, and a 25-V pulser for each element.

The conventional beamforming technique work as follows - prior to each transmit beam, the shift registers of each element is loaded with a single delay value. After all the elements are loaded with their respective delays, an external counter starts to count starting from 1 to the total number of firings. The comparator would then output a high when there is a match between

the stored delay value and the external counter. The comparator uses dynamic logic and the output high triggers the one-shot circuitry, which drives the on-chip pulser to fire a unipolar pulse. Therefore, by storing the appropriate delay values to each element, one can steer the ultrasound beam in space. The one-shot circuitry sets the pulse width of the high-voltage pulse and consists of a current-starved inverter chain. The pulse width is based on the operating frequency of the CMUT, which is 5 MHz. An off-chip current source controls the current-starved inverter chain and thus can be set to accommodate different CMUT operating frequencies. The on-chip pulser is adapted from the design described in [26].

On the receive end, each element consists of a transimpedance amplifier and an output buffer. The amplifier consists of a common source amplifier, a source follower buffer, and a 215-k Ω feedback resistor and provides a 3-dB bandwidth of 25-MHz. The output buffer is designed to drive capacitive loads of up to 50 pF and has an 800-mV peak-to-peak output swing for frequencies up to 10 MHz. A high-voltage switch protects the low-voltage receivers from the pulsers. The power consumption of each RX channel is 9 mW and the IC footprint measures 10 mm \times 6 mm [Fig. 3(b)].

B. 32 \times 32 IC

We designed another IC in a 0.25- μ m high-voltage process that can address a 32 \times 32 transducer array. Besides having four times as many number of channels, this IC has some improvements compared to the 16 \times 16 IC, e.g., the on-chip pulsers can generate a higher pulse voltage of up to 60 V, each RX channel consumes half as much power, and its footprint measures 9.2 mm \times 9.2 mm for four times the number of channels. The IC also has the provision for multi-beam transmit of up to four beams to improve the imaging frame rate. Lastly, this IC can provide a continuous-wave high-voltage pulse, useful for Doppler imaging and high intensity focused ultrasound (HIFU) applications. One advantage the 16 \times 16 IC has over this IC is the capability to perform photo-acoustic imaging due to the accessibility of receivers by each and every element. Every element in the 16 \times 16 IC has the ability to transmit and receive whereas for the 32 \times 32 IC, all elements outside the two diagonals have the capability to transmit while the 64 diagonal elements only have receive capability. This design choice for the 32 \times 32 IC was made to simplify the layout as it would not have been possible to put both the transmit and receive circuitry within a 250 μ m \times 250 μ m pitch. Table I provides a summary of the comparison between the two IC designs.

We use the 32 \times 32 IC for Assembly B and therefore, it was necessary to place the transmit or receive circuitry within the 250 μ m \times 250 μ m CMUT array pitch so as to perform direct flip-chip bonding with the CMUT array. In theory, it is only essential that the flip-chip pads on the IC align with the CMUT pads. However, not having the transmit or receive circuitry within the 250- μ m window would only make the interconnect network in the IC more complex.

Fig. 3(c) depicts the block diagram of the transmit and receive circuitry for a single element. Similar to the 16 \times 16 IC, this IC includes a transmit beamformer to enable focusing of an

TABLE I
IC DESIGN PROPERTIES

	16 \times 16 IC	32 \times 32 IC
Process node	1.5 μ m	0.25 μ m
Transmit element	256	960
Pulse voltage	25	60
Delay bit size	8 bit	10 bit
Multi-beam transmit	No	Yes
Receive element	256	64
RX channel gain	215 k Ω	200 k Ω
RX channel bandwidth	25 MHz	20 MHz
RX power / channel	9 mW	4.5 mW
Element pitch	250 μ m	250 μ m
Area	10 mm \times 6 mm	9.2 mm \times 9.2 mm

ultrasound wave in space. Each transmit element consists of a 40-bit shift register, a 10-bit comparator, a one-shot circuit and a high-voltage pulser. The 40-bit shift register is used to store up to four delay values of 10-bit each. Note the 2-bit increase in the number of bits per delay value as compared to the 16 \times 16 IC. This enables us to give better delay resolution allowing for a tighter focusing in space.

The shift registers of the elements in each row are connected in series, so the delays for the elements on each row are loaded serially. Therefore, we have 32 digital inputs corresponding to 32 IC rows, to set the delays for all array elements. These shift registers were designed to load at a rate of 100 MHz. The loading time had minimal effect on the imaging frame rate since it was negligible compared to the ultrasound time of flight.

The conventional beamforming technique of this IC work in a similar fashion as the 16 \times 16 IC, where prior to each transmit beam, the shift registers of each element is loaded with a single delay value. Zeros were loaded to the remaining three memory blocks in each element.

For simultaneous multi-beam transmit, instead of loading a single delay value, four delays are stored in each element (for a simultaneous transmit of four beams). When the first pulse fires, the comparator, in addition to triggering the one-shot circuitry, also triggers the internal 2-bit counter to change the memory location to the next delay value. The next pulse is fired based on the subsequent delay value and so on. As can be seen in the block diagram, the 2-bit counter can also be triggered externally by a global signal, if desired. The multi-beam feature has been tested in silicon. Fig. 6 shows the output of a single transmit element, loaded with four different delay values. What is shown are the output pulses of the pulser at those delay time. The test results also depict correct functionality of all the blocks in the transmit circuitry. The on-chip pulser (Fig. 4) is designed to have a rise and fall slew rate of about 1250 MV/sec for a 2.5 pF load (which is approximately the capacitance of the CMUT element). High-voltage transistors (marked by * in the figure) are used and have the capability of withstanding a high V_{DS} (up to 60 V).

Once the IC fires all the transmit beams, it goes into receive phase. In this phase, only the diagonal 64-elements are active. Each receive element consists of a transimpedance amplifier and an output buffer. The transimpedance amplifier uses a common source configuration. The amplifier and the buffer combined

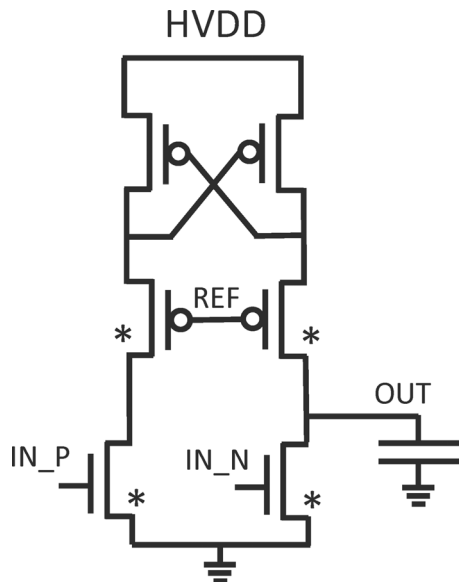


Fig. 4. High-voltage pulser design.

are designed to have a 3-dB bandwidth of 20 MHz and a transimpedance gain of 200 k Ω . For design of the amplifier, we modeled the CMUT using its equivalent circuit. Analytical expressions for the CMUT's response to pressure and voltage are used to obtain circuit parameter values for the model [21]–[23].

Since the receive circuitry is incorporated to improve the overall noise performance, it is imperative to design the amplifier with low noise. We achieved a simulated noise figure of 4.5 dB (at 5 MHz). Each receive channel consumes a power of 4.5 mW. Fig. 3(e) shows the die photo of the IC which measures 9.2 mm \times 9.2 mm. We have wire-bond pads only on two sides of the IC. This enables us to use this IC and tile four of them to form a larger 64 \times 64 array allowing for integration with an even larger CMUT array.

In our implementation of the transmit block, we designed the comparator to be self-resetting. The self-resetting nature enables the multi-beam transmit functionality of this chip. Also, by appropriately loading the delays to the element, and making sure the counter switches only between those delay values; one could generate a continuous-wave pulse in the element allowing for Doppler and high intensity focused ultrasound applications. This functionality of the IC is beyond the scope of this paper and is not discussed.

Our 32 \times 32 IC had an issue with IR drop when multiple pulsers fired. More specifically, when multiple pulsers fired, the IR drop in the high voltage line led to some of the pulsers (farthest end from the high-voltage pad) to see a lower voltage. This led to a variation in pulse width amongst different pulsers leading to a sub-optimal beamforming profile affecting the image quality in our imaging experiments. The issue has been corrected and a revised version of this IC has already been fabricated.

IV. 3-D INTEGRATION & ASSEMBLY

We use flip-chip bonding technology to interface the CMUT transducer and the IC, as large number of elements between the CMUT and IC need to interface and other techniques such as

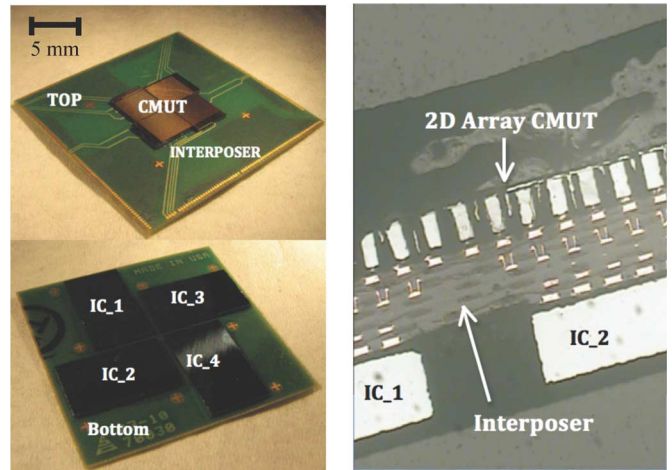


Fig. 5. Tiled CMUT array with ICs integrated with an interposer board (Assembly A). Cross-sectional view is shown on the right.

wire bonding is impractical. However, for such an approach, surface treatment of the IC pads is required.

The pads were first treated with Ni-Au under-bump metallization (UBM) using an electroless plating process. Then a solder jetting process was used to deposit solder balls of the IC. We chose a solder ball diameter of 80 μ m and a bump height of 50 μ m. Solder balls were also deposited on the topside of the interposer facing the CMUT array.

For integration, it was also important to probe each and every element of the CMUT array to look for shorts or non-working elements and then remove the corresponding solder ball from the IC. This ensures the functionality of the entire assembly even with few non-functional elements. We have probed all the elements of several 32 \times 32 CMUT arrays and were consistently observing a yield of >99%. In the future, we plan to incorporate switches between the CMUT and IC so that the switch in the appropriate element can be turned on/off as desired. Therefore, if a single element in the CMUT shorts after flip-chip bonding, the entire assembly can still function by turning off the switch of that element.

For Assembly A, we tile four 16 \times 16 CMUT arrays in a 2 \times 2 grid to form a larger 32 \times 32 CMUT array and flip-chip bond them to an interposer substrate. Polishing of the CMUT edges was required to achieve close to perfect tiling. The interposer used is a 6-layer substrate with a minimum trace width of 100 μ m and spacing of 50 μ m. On the backside, four 16 \times 16 ICs were flip-chip bonded to interface the 1024 CMUT elements. The entire assembly as well as the cross-section is illustrated in Fig. 5.

For Assembly B, the larger 32 \times 32 CMUT array is directly flip-chip bonded to a 32 \times 32 IC. The flip-chip bonding was performed using an in-house flip-chip bonder where the IC and the CMUT array were aligned with respect to each other and bonded under high pressure and temperature. Fig. 7 illustrates the assembly. For both assemblies, under filling was performed to provide mechanical stability.

V. IMAGING SETUP AND CHARACTERIZATION

Figs. 8 and 9 illustrate the experimental setup. The CMUT-IC assembly is placed and wire bonded onto a substrate, which

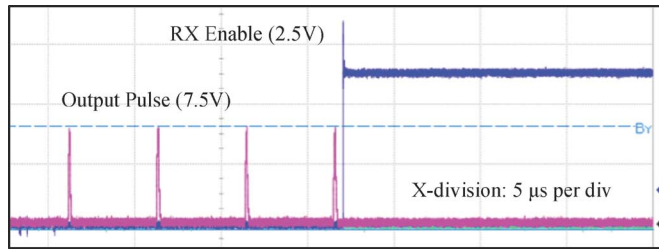


Fig. 6. Multiple pulses per element. Pulse voltage set to 7.5 V for testing purposes.

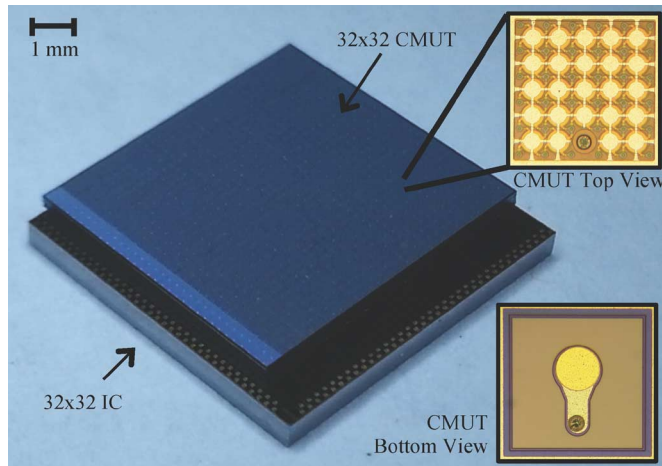


Fig. 7. Assembly B (32×32 CMUT array integrated with 32×32 IC).

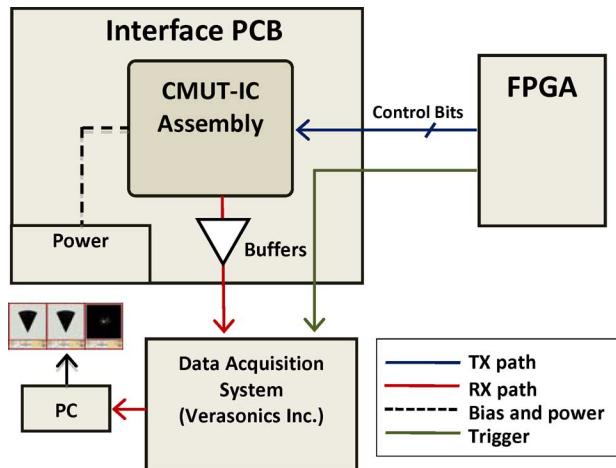


Fig. 8. Imaging setup block diagram.

plugs into the interface board. The interface board provides necessary biasing to the IC, off-chip buffers for the RF channels and level-shifters for the digital I/O signals. The FPGA is programmed to calculate transmit delays and control the IC for transmit beamforming. The RF data received from the CMUT array are signal conditioned and sampled by a programmable data acquisition system (Verasonics data acquisition system, Verasonics Inc., Redmond, WA), and then processed by custom real-time imaging software [27]. To obtain an image frame, one requires multiple data acquisitions, the number of which equals the number of scan lines in the volume of interest. Each data acquisition consists of a delay loading phase, a transmit phase

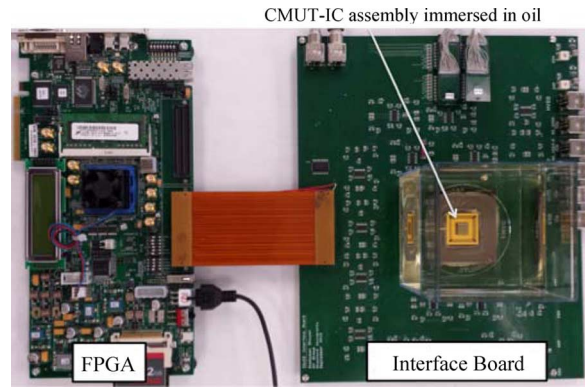


Fig. 9. Illustration of our imaging system.

TABLE II
HYDROPHONE MEASUREMENTS (2.4 MM AWAY FROM CMUT SURFACE)

Pulse Voltage (V)	CMUT Bias (V)	Measured Pressure (KPa)
25	31	51
30	29	62
35	26	71
40	29	84
45	31	94
50	35	102
55	34	112

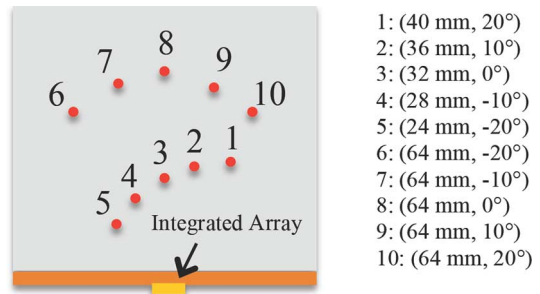


Fig. 10. Wire targets (location with respect to CMUT array).

and a receive phase. Custom imaging software reconstructs the volume through conventional delay-and-sum beamforming, and displays a real-time volume-rendered image along with three cross-sectional images on the screen.

Before performing imaging experiments, we performed some hydrophone measurements to characterize the achievable output pressure for different combinations of the CMUT DC bias and the pulse excitation voltage for a single element of the 32×32 CMUT array (Assembly B). Table II summarizes the output pressure measured by the hydrophone located 2.4 mm away from the surface of the CMUT element. Using a mathematical model [28], we calculated the peak-to-peak pressure observed at the surface, accounting for attenuation and diffraction losses. The maximum peak-to-peak pressure observed at the surface is approximately 1.4 MPa (with diffraction being the major source of loss).

VI. IMAGING EXPERIMENTS AND TESTING

We performed initial imaging experiments on nylon wire targets with a diameter of $300 \mu\text{m}$ (Fig. 10), a metal spring target,

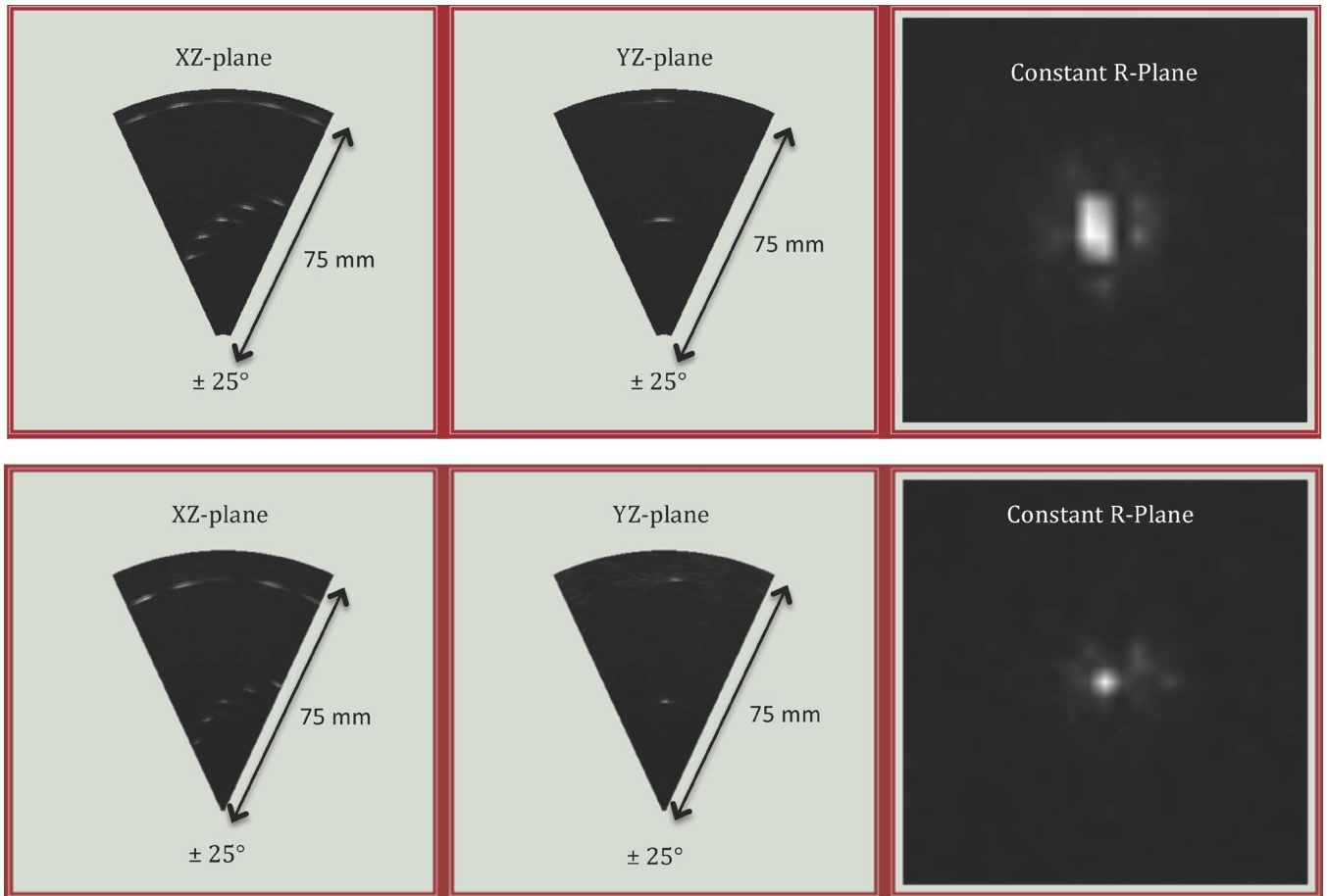


Fig. 11. Real-time imaging results in three planes for Assembly A (top) and Assembly B (bottom).

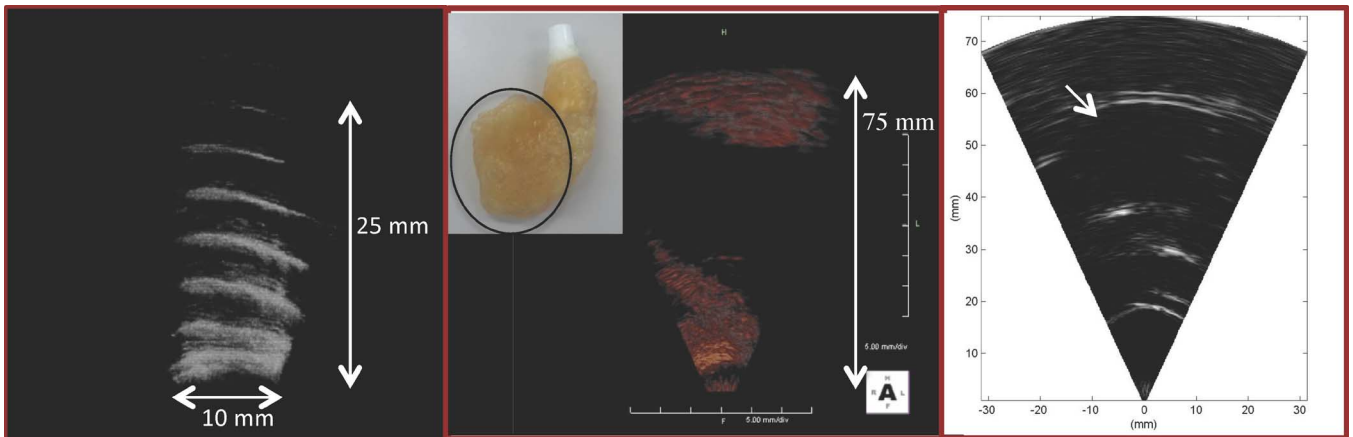


Fig. 12. Volume rendered images of spring target (left) and ventricle model (middle). B-mode image of prostate phantom (right). Images acquired using Assembly A.

a ventricle model, and a human prostate (ex-vivo). A tank was built to test the assembly in vegetable oil. All our imaging experiments were performed with a 25-V pulse and CMUT bias of 30 V. The conventional phase array beamforming was used to reconstruct these images. Figs. 11 and 12 show the imaging results. With an imaging depth of 75 mm, we could achieve an imaging rate of 5 volumes per second for displaying three cross-sectional images. This frame rate was limited by the data transfer, via a PCI express interface, from the Verasonics data

acquisition system to the PC. When we also display a volume-rendered image, the computation load in signal processing further reduces the frame rate to 3 volumes per second.

VII. CONCLUSION

We demonstrated a 3-D ultrasound imaging system that is capable of displaying real-time volumetric images at 3–5 volumes per second. Front-end electronics were designed and integrated with CMUTs to mitigate the various challenges in de-

veloping such a system. The electronics consisted of a transmit beamformer and low-noise amplifiers and were integrated with the CMUT array either with a help of an interposer or by direct flip-chip bonding. Imaging experiments were performed with several phantoms such as a wire, spring, ventricle model and a human prostrate. More imaging experiments are ongoing with Assembly B using the multi-beam transmit feature of the 32×32 IC. Future work also includes development of a system that is capable of providing simultaneous HIFU and imaging capabilities.

ACKNOWLEDGMENT

The authors would like to thank National Semiconductor and Intersil Corporation for their valuable support in the design and fabrication of the IC. CMUT fabrication was done at the Stanford Nanofabrication Facility (Stanford, CA, USA), a member of National Nanotechnology Infrastructure Network. They would also like to thank P. Prather for her support during wire-bonding and assembly, and Verasonics for its programming support.

REFERENCES

- [1] L. F. Goncalves, W. Lee, J. Espinoza, and R. Romero, "Three- and 4-dimensional ultrasound in obstetric practice: Does it help?," *J. Ultrasound Med.*, vol. 24, no. 12, pp. 1599–1624, 2005.
- [2] B. R. Benacerraf, T. D. Shipp, and B. Bromley, "Three-dimensional US of the fetus: Volume imaging," *Radiology*, vol. 238, no. 3, pp. 988–996, 2006.
- [3] A. Fenster, D. B. Downey, and H. N. Cardinal, "Three-dimensional ultrasound imaging," *Phys. Med. Biol.*, vol. 46, no. 5, p. R67, 2001.
- [4] S. W. Smith, H. R. Pavy, and O. T. von Ramm, "High-speed ultra-sound volumetric imaging system. I. Transducer design and beam steering," *IEEE Trans. Ultrason., Ferroelectr., Freq. Control*, vol. 38, no. 2, pp. 100–108, 1991.
- [5] L. F. Goncalves, J. Espinoza, J. P. Kusanovic, W. Lee, J. K. Nien, J. Santolaya-Forgas, G. Mari, M. C. Treadwell, and R. Romero, "Applications of 2-dimensional matrix array for 3- and 4-dimensional examination of the fetus: A pictorial essay," *J. Ultrasound Med.*, vol. 25, no. 6, pp. 745–755, 2006.
- [6] I. Wygant, X. Zhuang, D. Yeh, Ö. Oralkan, A. Ergun, M. Karaman, and B. T. Khuri-yakub, "Integration of 2-D CMUT arrays with front-end electronics for volumetric ultrasound imaging," *IEEE Trans. Ultrason., Ferroelectr., Freq. Control*, vol. 55, no. 2, pp. 327–342, 2008.
- [7] A. Bhuyan, J. W. Choe, B. C. Lee, P. Cristman, Ö. Oralkan, and B. T. Khuri-Yakub, "Miniaturized, wearable, ultrasound probe for on-demand ultrasound screening," in *Proc. IEEE Ultrasonics Symp.*, 2011, vol. 1.
- [8] A. Nikoozadeh, Ö. Oralkan, M. Gencel, J. W. Choe, D. N. Stephens, A. de la Rama, P. Chen, K. Thomenius, A. Dentinger, D. Wildes, K. Shivkumar, A. Mahajan, M. O'Donnell, D. Sahn, and P. T. Khuri-Yakub, "Forward-looking volumetric intracardiac imaging using a fully integrated CMUT ring array," in *Proc. IEEE Ultrasonics Symp.*, 2009, pp. 511–514.
- [9] J. V. Hatfield and K. S. Chai, "A beam-forming transmit ASIC for driving ultrasonic arrays," *Sens. Actuators A*, vol. 92, no. 1–3, pp. 273–279, 2001.
- [10] I. G. Mina, H. Kim, I. Kim, S. K. Park, K. Choi, T. N. Jackson, R. L. Tutwiler, and S. Trolrier-McKinstry, "High frequency piezoelectric MEMs ultrasound transducers," *IEEE Trans. Ultrason., Ferroelectr., Freq. Control*, vol. 54, no. 12, pp. 2422–2430, 2007.
- [11] T. Halvorsrod, W. Luzzi, and T. S. Lande, "A log-domain μ beamformer for medical ultrasound imaging systems," *IEEE Trans. Circuits Syst. I, Reg. Papers*, vol. 52, no. 12, pp. 2563–2575, 2005.
- [12] B. Stefanelli, I. O'connor, L. Quiquerez, A. Kaiser, and D. Billet, "An analog beam-forming circuit for ultrasound imaging using switched current delay lines," *IEEE J. Solid-State Circuits*, vol. 35, no. 2, pp. 202–211, 2000.
- [13] M. Vaowu, T. Tanaka, S. Arita, A. Tsuchitani, K. Inoue, and Y. Suzuki, "Pipelined delay-sum architecture based on bucket-brigade devices for on-chip ultrasound beamforming," *IEEE J. Solid-State Circuits*, vol. 38, no. 10, pp. 1754–1757, 2003.
- [14] J. R. Talman, S. L. Garverick, and G. R. Lockwood, "Integrated circuit for high-frequency ultrasound annular array," in *Proc. IEEE Custom Integrated Circuits Conf.*, 2003, pp. 477–480.
- [15] J. R. Talman, S. L. Garverick, C. E. Morton, and G. R. lockwood, "Unit-delay focusing architecture and integrated-circuit implementation for high-frequency ultrasound," *IEEE Trans. Ultrason., Ferroelectr., Freq. Control*, vol. 50, no. 11, pp. 1455–1463, 2003.
- [16] K. Kaviani, Ö. Oralkan, B. T. Khuri-Yakub, and B. Wooley, "A multichannel pipeline analog-to-digital converter for an integrated 3-d ultrasound imaging system," *IEEE J. Solid-State Circuits*, vol. 38, no. 7, pp. 1266–1270, 2003.
- [17] C. Daft, S. Calmes, D. Da Graca, K. Patel, P. Wagner, and I. Ladabaum, "Microfabricated ultrasonic transducers monolithically integrated with high voltage electronics," in *Proc. IEEE Ultrasonics Symp.*, 2004, vol. 1, pp. 493–496.
- [18] I. Wygant, N. Jamal, H. Lee, A. Nikoozadeh, Ö. Oralkan, M. Karaman, and B. T. Khuri-Yakub, "An integrated circuit with transmit beamforming flip-chip bonded to a 2-D CMUT array for 3-D ultrasound imaging," *IEEE Trans. Ultrason., Ferroelectr., Freq. Control*, vol. 56, no. 10, pp. 2145–2156, 2009.
- [19] I. Wygant, M. Karaman, Ö. Oralkan, and B. K. Yakub, "Beamforming and hardware design for a multichannel front-end integrated circuit for real-time 3-D catheter-based ultrasonic imaging," in *Proc. SPIE Medical Imaging*, San Diego, CA, USA, 2006, vol. 6147.
- [20] A. S. Erguri, Y. Huang, X. Zhuang, Ö. Oralkan, G. G. Yarahoglu, and B. T. Khuri-Yakub, "Capacitive micromachined ultrasonic transducers: Fabrication technology," *IEEE Trans. Ultrason., Ferroelectr., Freq. Control*, vol. 52, no. 12, pp. 2242–2258, 2005.
- [21] A. Nikoozadeh, B. Bayram, G. Yarioluglu, and B. T. Khuri-yakub, "Analytical calculation of collapse voltage of cMUT membrane [capacitive micromachined ultrasonic transducers]," in *Proc. IEEE Ultrasonics Symp.*, 2004, vol. 1, pp. 256–259.
- [22] I. Ladabaum, J. Xuecheng, H. T. Soh, A. Atalar, and B. T. Khuri-yakub, "Surface micromachined capacitive ultrasonic transducers," *IEEE Trans. Ultrason., Ferroelectr., Freq. Control*, vol. 45, no. 3, pp. 678–690, 1998.
- [23] A. Lohfink and P. C. Eccardt, "Linear and nonlinear equivalent circuit modeling of cMUTs," *IEEE Trans. Ultrason., Ferroelectr., Freq. Control*, vol. 52, no. 12, pp. 2163–2172, 2005.
- [24] C. H. Cheng, A. Ergun, and B. T. Khuri-yakub, "Electrical through-wafer interconnects with 0.05 picofarads parasitic capacitance on 400- μ m thick silicon substrates," in *Proc. Solid-State Sensor and Actuator Workshop*, Hilton Head Island, SC, USA, 2002.
- [25] X. Zhuang, I. O. Wygant, D. S. Lin, M. Kupnik, Ö. Oralkan, and B. T. Khuri-yakub, "Trench-isolated cMUT arrays with a supporting frame: Characterization and imaging results," in *Proc. IEEE Ultrasonics Symp.*, 2007, pp. 507–510.
- [26] M. Declercq, M. Schubert, and F. Clement, "5 V-to-75 V CMOS output interface circuits," in *Proc. IEEE Int. Solid-State Circuits Conf.*, 1993, pp. 162–163, 283.
- [27] J. W. Choe, Ö. Oralkan, A. Nikoozadeh, A. Bhuyan, B. C. Lee, M. Gencel, and B. T. Khuri-Yakub, "Real-time volumetric imaging system for CMUT arrays," in *Proc. IEEE Ultrasonics Symp.*, 2011.
- [28] G. S. Kino, *Acoustic Waves: Devices, Imaging, and Analog Signal Processing*. Englewood Cliffs, NJ: Prentice-Hall, 1987.
- [29] A. Bhuyan, J. W. Choe, B. C. Lee, I. Wygant, A. Nikoozadeh, Ö. Oralkan, and B. T. Khuri-Yakub, "3D volumetric ultrasound imaging with a 3232 CMUT array integrated with front-end ICs using flip-chip bonding technology," in *Proc. IEEE Int. Solid-State Circuits Conf. Dig. Tech. Papers*, Feb. 2013, pp. 396–397.
- [30] A. Bhuyan, C. Chang, J. W. Choe, B. C. Lee, A. Nikoozadeh, Ö. Oralkan, and B. T. Khuri-Yakub, "A 32×32 integrated CMUT array for volumetric ultrasound imaging," in *Proc. IEEE Ultrasonics Symp.*, 2013.
- [31] R. Wodnicki, C. G. Woychik, A. T. Byun, R. Fisher, K. Thomenius, D. S. Lin, X. Zhuang, Ö. Oralkan, S. Vaithilingam, and B. T. Khuri-Yakub, "Multi-row linear CMUT array using CMUTs and multiplexing electronics," presented at the IEEE Ultrasonics Symp., Rome, Italy, Sept. 2009.
- [32] M. Wang and J. Chen, "Volumetric flow measurement using an implantable CMUT array," *IEEE Trans. Biomed. Circuits Syst.*, vol. 5, no. 3, pp. 214–222, Jun. 2011.



Anshuman Bhuyan (S'04) received the B.S.E. degree from the University of Michigan, Ann Arbor, MI, USA, and the M.S. degree from Stanford University, Stanford, CA, USA, both in electrical engineering, in 2006 and 2008, respectively.

He is working toward the Ph.D. degree in the electrical engineering department at Stanford University. He has previously held internship positions in the ASIC group at Texas Instruments, Dallas, TX, MEMS design group at Analog Devices, Cambridge, MA, USA, and the mixed-signal IC design group at Rambus, Los Altos, CA, USA. He has also worked on reliability (NBTI degradation) of transistors and circuit techniques to detect them, while pursuing the M.S. degree. His research interests include analog, mixed-signal IC design and interface circuits for MEMS devices. Currently, he is working as a Research Assistant in the Khuri-Yakub Ultrasonics Group and is involved in the front-end electronics for the volumetric ultrasound imaging project.



Jung Woo Choe (S'10) received the B.S. degree from Seoul National University (SNU), Seoul, Korea, and the M.S. degree from Stanford University, Stanford, CA, USA, both in electrical engineering, in 2005 and 2008, respectively.

He is working toward the Ph.D. degree in electrical engineering at Stanford University. He was awarded the General Electric Fellowship while at SNU, and the Kwanjeong Educational Foundation Fellowship from 2006 to 2011. He worked as a Programmer at Spire Technology Inc., Anyang, Korea, from 2002 to 2003, and at NHN Cooperation, Seoul, Korea, from 2003 to 2005. He is now working as a Research Assistant at Edward L. Ginzton Laboratory, Stanford University. His research interests include design and implementation of real-time volumetric ultrasound imaging systems for capacitive micromachined ultrasonic transducer (CMUT) arrays, and software development for those systems.



Byung Chul (B. C.) Lee (S'03) received the B.S. degree in electrical engineering (Summa Cum Laude) from Korea University, Seoul, Korea, and the M.S. degree in electrical engineering from the Korea Advanced Institute of Science and Technology (KAIST), Daejeon, Korea, in 2003 and 2005, respectively.

He is working toward the Ph.D. degree in electrical engineering at Stanford University, Stanford, CA, USA. He has worked at the Korea Institute of Science and Technology (KIST), Seoul, Korea, since receiving the M.S. degree. While at KIST, he worked as a Research Scientist in MEMS and NEMS technology for many biomedical applications such as nanobiosensors, neural probes, and fast DNA sequencing devices. His current research interests include MEMS/NEMS technology and medical ultrasound applications with novel CMUT structures.



Ira O. Wygant (S'98–M'10) received the B.S. degree from the University of Wyoming, Laramie, WY, USA, and the M.S. and Ph.D. degrees from Stanford University, Stanford, CA, USA, all in electrical engineering, in 1999, 2002, and 2008, respectively.

Currently, he is a MEMS engineer at Texas Instrument's Kilby Labs. His research interests include MEMS ultrasonic transducers and their applications.



Amin Nikoozadeh (S'03–M'11) received the B.S. degree from the Sharif University of Technology, Tehran, Iran, and the M.S. and Ph.D. degrees from Stanford University, Stanford, CA, USA, all in electrical engineering, in 2002, 2004, and 2010, respectively.

While working on the Ph.D. degree, he designed and developed fully-integrated ultrasound imaging catheters for forward-viewing intracardiac imaging using capacitive micromachined ultrasonic transducers (CMUTs). In 2011, he joined the E. L. Ginzton Laboratory at Stanford University as a Research Associate. His past and present research interests include medical ultrasound imaging, image-guided therapeutics, MEMS, and analog circuit design, with a main focus on design, modeling, fabrication and integration of CMUTs. His current research focuses on the implementation of fully-integrated CMUT arrays for catheter-based ultrasound imaging, real-time volumetric ultrasound imaging using 2-D CMUT arrays with integrated electronics, high-intensity focused ultrasound (HIFU) therapy, low-intensity ultrasound for neurostimulation applications, photo-acoustic imaging, and novel ultrasound transducer technologies.



Ömer Oralkan (S'93–M'05–SM'10) received the B.S. degree from Bilkent University, Ankara, Turkey, the M.S. degree from Clemson University, Clemson, SC, USA, and the Ph.D. degree from Stanford University, Stanford, CA, USA, all in electrical engineering, in 1995, 1997, and 2004, respectively.

He was a Research Associate (2004–2007) and then a Senior Research Associate (2007–2011) in the E. L. Ginzton Laboratory at Stanford University, and an Adjunct Lecturer (2009–2011) in the Department of Electrical Engineering at Santa Clara University, Santa Clara, CA, USA. In 2012, he joined the Department of Electrical and Computer Engineering, North Carolina State University, Raleigh, NC, USA, as an Associate Professor. His current research focuses on developing devices and systems for ultrasound imaging, photoacoustic imaging, image-guided therapy, biological and chemical sensing, and ultrasound neural stimulation. He has authored more than 130 scientific publications.

Dr. Oralkan is an Associate Editor for the IEEE TRANSACTIONS ON ULTRASONICS, FERROELECTRICS AND FREQUENCY CONTROL and serves on the Technical Program Committee of the IEEE Ultrasonics Symposium. He received the 2013 DARPA Young Faculty Award and the 2002 Outstanding Paper Award of the IEEE Ultrasonics, Ferroelectrics, and Frequency Control Society.



Butrus (Pierre) T. Khuri-Yakub (S'70–M'76–SM'87–F'95) received the B.S. degree from the American University of Beirut, Beirut, Lebanon, the M.S. degree from Dartmouth College, Hanover, NH, USA, and the Ph.D. degree from Stanford University, Stanford, CA, USA, all in electrical engineering.

He is a Professor of Electrical Engineering at Stanford University. His current research interests include medical ultrasound imaging and therapy, ultrasound neuro-stimulation, chemical/biological sensors, gas flow and energy flow sensing, micro-machined ultrasonic transducers, and ultrasonic fluid ejectors. He has authored more than 550 publications and has been principal inventor or coinventor of 92 U.S. and international issued patents.

Dr. Khuri-Yakub was awarded the Medal of the City of Bordeaux in 1983 for his contributions to Nondestructive Evaluation, the Distinguished Advisor Award of the School of Engineering at Stanford University in 1987, the Distinguished Lecturer Award of the IEEE UFFC Society in 1999, a Stanford University Outstanding Inventor Award in 2004, Distinguished Alumnus Award of the School of Engineering of the American University of Beirut in 2005, Stanford Biodesign Certificate of Appreciation for commitment to educate, mentor and inspire Biodesign Fellows, 2011, and 2011 recipient of the IEEE Rayleigh Award.